Capacity Requirements in Networks of Quantum Repeaters and Terminals

Michel Barbeau
School of Computer Science
Carleton University
Ottawa, Ontario, Canada
iD 0000-0003-3531-4926

Joaquin Garcia-Alfaro
Institut Polytechnique de Paris
SAMOVAR, Telecom SudParis
Paris, France
iD 0000-0002-7453-4393

Evangelos Kranakis
School of Computer Science
Carleton University
Ottawa, Ontario, Canada
iD 0000-0002-8959-4428

Abstract—We consider the problem of path congestion avoidance in networks of quantum repeaters and terminals. In other words, the avoidance of situations when demands exceed capacity. We assume networks in which the sets of complete paths between terminals may affect the capacity of repeaters in the network. We compare the reduction of congestion avoidance of two representative path establishment algorithms: shortest-path establishment vs. layer-peeling path establishment. We observe that both strategies provide an equivalent entanglement rate, while the layer-peeling establishment algorithm considerably reduces the congestion in the network of repeaters. Repeaters in the inner layers get less congested and require a lower number of qubits, while providing a similar entanglement rate.

Index Terms—Quantum network, quantum communication, quantum repeater, entanglement swapping, entanglement routing, entanglement distribution

I. Introduction

Quantum networking aims at routing and forwarding of quantum information from one node to another. Envisioned applications include distributed quantum computing in general and more specific domains such as distributed quantum machine learning. In future quantum networks, it is foreseen that quantum teleportation and quantum repeaters [1], [2], [3] will be key building blocks [4], [5], [6]. Teleportation is a protocol devised to transfer a qubit from one location to another, but they must share entanglement [7]. When connected by a quantum channel, entanglement can be directly established between two locations. If not, then entanglement distribution is required. Entanglement distribution relies on entanglement swapping [8]. Leveraging entanglement distribution, possibly with purification and error correction, quantum repeaters are the network elements envisioned for routing in quantum networks [9].

In a quantum network consisting of repeaters and terminals, we are interested in analyzing the capacity required at repeaters by paths connecting all pairs of terminals. We investigate the following specific question: What is the required quantum memory size (in qubits) in repeaters to interconnect all terminals with each other?

We define a quantum network model, making the distinction between repeaters and terminals. Interconnected repeaters achieve the core of the networks while terminals are on its periphery. We assume that all terminals need to be interconnected with each other to exchange quantum data. We develop lower and upper bounds for the required qubit memory size of repeaters for general graphs and two-dimensional grid network topologies. We define the layer peeling algorithm for routing quantum connections. It is compared with shortest-path routing w.r.t. congestion and entanglement rate.

Related work is reviewed in Section II. Our network model in presented in Section III. Quantum networks with general graph topologies are analyzed in Section IV. Two-dimensional grid quantum networks are examined in Section V. We conclude with Section VII.

II. Related Work

This article focuses on the quantity of quantum memory required by repeaters performing entanglement distribution. Presented in detail in Section III-B, our model is consistent with the quantum repeater protocol used by several authors [10]. We assume that repeaters build upon the entanglement swapping operation [8], where quantum memory is required to store qubits entangled with qubits stored in other network nodes. An alternative is the all-photonic quantum repeater model of Azume et al. [11], [12].

There are two related problems: entanglement routing and entanglement distribution. Given a source and a destination, entanglement routing finds a path connecting the two endpoints [13], [14], [15], [16]. Analogous to packet forwarding in classical networks, entanglement distribution performs a sequence of swaps to transfer a quantum state [17], [18], [19]. Using the route between the source and destination, entanglement swapping is executed step-by-step to transfer quantum information between the two network end points. In this context, it is reasonable to assume that repeaters are imperfect [10]. This translates to probabilities of entanglement pair creation and entanglement swapping success. Entanglement routing has been studied for specific network topologies. There are works with a focus on linear [20], [21], [17], grid [15], ring [19], [22] or sphere [19] topologies, in which the size of the required quantum memory is related to the number of neighbors that a repeater has.

In this article, we address issues related to qubit capacity of repeaters, i.e., the required number of qubits that quantum repeaters need to maintain entanglement between multiple quantum network-edge terminals. The main issue is how to select a set of paths that optimizes the capacity induced on the graph representing a network of quantum repeaters and terminals. Most of the past works study the entanglement generation rate between two peers, over a quantum network. In contrast, we study networks with multiple peers, a situation generating multiple paths. In our model, the amount of required quantum memory is proportional to the number of paths traversing a repeater, see Definition 2. Several related papers use routing metrics such as entanglement rate and shortest path. In this paper, we assume that links are uniform and have the same

entanglement rate. We show that the shortest path metric is not the one that optimizes the capacity of a quantum network.

III. NETWORK MODEL

We present our quantum network and repeater models.

A. Topology Model

Consider a graph G with vertex set V and edge set E. Assume that the set V of vertices is partitioned into two distinct sets R and T such that $V = R \cup T$. R is the set of *repeaters*. T is the set of *terminals*. A graph G with its two
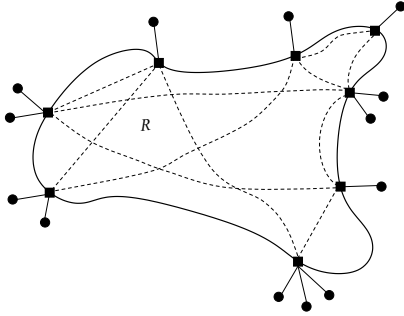

Fig. 1. Disk vertices are terminals in T. Squares are repeaters in R. Terminals are directly connected to repeaters. A dashed line represents a path consisting of repeaters; the endpoints of the path connect terminals.

sets of repeaters and terminals is denoted by $G = (R, T, E)$, see Fig. 1. An edge represents a bi-directional quantum channel, which can be used to establish entanglement between its two end-points. All repeaters and terminals have limited quantum memory and can perform entanglement swapping, see Section III-B. Consider the path $p = v_0, v_1, \ldots, v_{s-1}, v_s$ of vertices in V such that the start and final vertices v_0, v_s are terminals in T, while all its intermediate vertices $v_i \in R$, $0 < i < s$ are repeaters in R. Note that such a path consists of $s+1$ nodes two of which are terminals, namely v_0, v_s, and $s-1$ are repeaters, namely $v_1, v_2, \ldots, v_{s-1}$.

Definition 1 (Complete Set of Paths). *A set P of paths is called* complete *if for any two terminal pair $t, t' \in T$ there is a path $p = v_0, v_1, \ldots, v_{s-1}, v_s \in P$ such that $t = v_0, t' = v_s$ and all intermediate vertices are repeaters in R.*

We require that:

- terminal nodes are not adjacent to each other in the graph,
- every terminal node is adjacent to at least one repeater, and
- repeater nodes can communicate directly with each other if they are adjacent in the graph.

Definition 2 (Capacity of a Repeater). *For a given complete set of paths P in a graph $G = (R, T, E)$ and any repeater $r \in R$ let the capacity of r, denoted by $C_P(r)$ be defined as the number of paths $p \in P$ that pass through r, see Fig. 2.*

The intuition behind this definition is that the capacity of a repeater is proportional to the number of qubits it must be able to store, paired with entanglement, so as to make possible communication between terminals.

Definition 3 (Capacity Induced by a Complete Set of Paths). *For a given complete set of paths P in a graph $G = (R, T, E)$,*
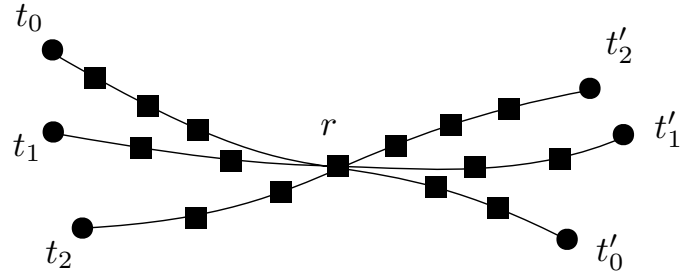

Fig. 2. The capacity of a repeater r is the number of paths that go through r; in the picture this is equal to three. Note that the squares depict repeaters (from the set R) and disks terminals (from the set T).

the capacity of $G = (R, T, E)$ induced by the complete set of paths P is defined as the maximum capacity caused by repeaters in R and is defined by the formula

$$C_G(P) := \max_{r \in R} C_P(r) \; qubits, \tag{1}$$

Let $\mathcal{P}_G$ denote the set of complete sets of paths P for the graph $G = (R, T, E)$ of repeaters and terminals. When this is easily understood from the context, we may omit the subscript G from $\mathcal{P}_G$. Among the collections of complete set of paths for the graph G, we are interested in minimizing the quantity $C_G(P)$, namely

$$\min_{P \in \mathcal{P}_G} C_G(P) = \min_{P \in \mathcal{P}_G} \max_{r \in R} C_P(r) \; qubits, \tag{2}$$

where the minimum is taken over the set $\mathcal{P}_G$ of all possible complete sets of paths P for the graph $G = (R, T, E)$.

The main problem arising concerns the capacity caused by connecting all pairs of terminals by paths consisting of repeaters. We are aiming for an algorithm that defines the set of paths P and at the same time minimizes the resulting capacity induced on the graph. The main problem can be described as follows.

Problem 4. *Given a graph $G = (R, T, E)$ whose set of repeaters is R and set of terminals is T, find a complete set of paths P that attains or approximates the quantity $\min_{P \in \mathcal{P}_G} C_G(P)$.*

This capacity is to be interpreted as the number of qubits the repeaters would need to store so as to make possible communication between terminals using qubits.

B. Repeater Model

In this sub-section, we describe a model of quantum repeaters. Acknowledging their imperfection, we define a qubit error model. Next, we explain the use of purification to improve the fidelity of quantum data. Finally, we discuss entanglement swapping, the main functionality of a quantum repeater, and the associated cost in terms of quantum memory. Entanglement swapping establishes Bell-EPR pairs between them, which in turn enables teleportation of quantum data between terminals, and eventually other operations.

The basic purification procedure deals with errors in qubit pairs, see Chapter 8 in [5]. Let us consider a simple error

model in which solely single qubit errors are relevant.[1] For example, in the following pair, as for any Bell-EPR pair

$$|\psi\rangle = \frac{|00\rangle + |11\rangle}{\sqrt{2}}. \tag{3}$$

when both qubits are inverted, the errors are cancelled, the term $|00\rangle$ becomes $|11\rangle$ and vice versa. However, the presence of a single qubit error results into the pair

$$|\phi\rangle = \frac{|01\rangle + |10\rangle}{\sqrt{2}}. \tag{4}$$

Let us say the first qubit flips, the term $|00\rangle$ becomes $|10\rangle$ and the term $|11\rangle$ becomes $|01\rangle$. Note the result is the same when the second qubit flips. Let $\beta \in [0, 1]$ be the probability of a single qubit inversion error. The probability of no error, denoted as α, is then equal to $1 - \beta$. The error model is represented as the quantum state

$$\sqrt{\alpha}\,|\psi\rangle + \sqrt{\beta}\,|\phi\rangle. \tag{5}$$

The concept of *fidelity* refers to the degree of resemblance of a quantum state to its original value. Errors affect fidelity. The establishment of high fidelity Bell-EPR pairs between nodes is a core quantum networking functionality. Purification is a procedure executed between two nodes, Alice and Bob, to achieve fidelity. It is assumed that they share two Bell-EPR pairs $|\psi\rangle_A$ and $|\psi\rangle_B$. During the purification process, one pair is sacrificed for the benefit of increased fidelity in the other. Let the pairs $|\psi\rangle_A$ and $|\psi\rangle_B$ both be defined as $|\Phi^+\rangle = \frac{|00\rangle + |11\rangle}{\sqrt{2}}$. From the pair $|\psi\rangle_A$, the first qubit $|\psi_1\rangle_A$ is dispatched to Alice. The second qubit $|\psi_2\rangle_A$ is dispatched to Bob. From the pair $|\psi\rangle_B$, the first qubit $|\psi_1\rangle_B$ is dispatched to Alice. The second qubit $|\psi_2\rangle_B$ is dispatched to Bob. During the dispatch, qubit errors can be introduced. Therefore, Alice gets a pair $|\psi_1'\rangle_A |\psi_1'\rangle_B$. She applies a $CNOT$ gate yielding the pair

$$|\phi\rangle = CNOT\left(|\psi_1'\rangle_A |\psi_1'\rangle_B\right).$$

Similarly, Bob gets a pair $|\psi_2'\rangle_A |\psi_2'\rangle_B$. He applies a $CNOT$ gate yielding the pair

$$|\sigma\rangle = CNOT\left(|\psi_2'\rangle_A |\psi_2'\rangle_B\right).$$

Alice measures her second qubit, i.e, $|\phi_2\rangle$, resulting into a classical bit (cbit) z_1. Bob measures his second qubit, i.e, $|\sigma_2\rangle$, yielding cbit z_2. Using classical communications, Alice and Bob compare the values of z_1 and z_2. When they are equal, it is concluded that the pair $|\phi_1\rangle |\sigma_1\rangle$, i.e., the first qubits of $|\phi\rangle$ and $|\sigma\rangle$, has been purified and corresponds to the state $|\Phi^+\rangle$. It is used. When z_1 and z_2 are different, it is concluded that the pair $|\phi_1\rangle |\sigma_1\rangle$ is not equal to $|\Phi^+\rangle$. Purification failed. The pair $|\phi_1\rangle |\sigma_1\rangle$ is rejected.

There are four possible purification outcomes. When z_1 is equal to z_2, there are two cases. There are no errors and both pairs are in state $|\psi\rangle$ (Equation (3)). Or, both pairs are in error and in state $|\phi\rangle$ (Equation (4)). The probability of the former case is α^2. Purification has been conducted with success. The probability of the latter case is β^2. The errors are undetected. Purification wrongly concludes with success. When z_1 and z_2 are different, it is because there is a qubit error in one of the

pairs. Either pair $|\psi'\rangle_A$ or pair $|\psi'\rangle_B$ is in state $|\phi\rangle$, but not both. The probability for the first or second pair to be in error is $\alpha\beta$. In both cases, the error is detected. Purification fails. The pair $|\phi_1\rangle |\sigma_1\rangle$ is not used.

In this setting, as a function of the error probability β, fidelity becomes equivalent to the probability of the absence of errors when purification concludes with a positive result, that is:

$$f(\beta) = \frac{\alpha^2}{\alpha^2 + \beta^2} \text{ with } \alpha = 1 - \beta \tag{6}$$

We assume that adjacent nodes, repeaters and terminals, can use direct communications to establish entanglement. A quantum repeater establishes a Bell-EPR pair between two repeaters, two terminals or a repeater and a terminal that are distant, i.e., no adjacent. The fidelity of the Bell-EPR pair may be increased with purification. The terminals do not need to share a priori a Bell-EPR pair. Each terminal however, needs to share a Bell-EPR pair with a third-party repeater that plays a *hub* role. To create entanglement between the two parties, a repeater uses entanglement swapping. Fig. 3 pictures a circuit for entanglement swapping. There are three network nodes involved: a source, an intermediate and a destination. The top- and bottom-left rectangles represent two Bell-EPR pair production sub-circuits. Because the two input qubits to these sub-circuits are both $|0\rangle$, the Bell-EPR pairs that are produced are both $|\Phi^+\rangle$. One qubit of the first Bell-EPR pair (top-line) is dispatched to the source. The other qubit of this first Bell-EPR pair (second line) is dispatched to the intermediate. One qubit of the second Bell-EPR pair (third line) is dispatched to the intermediate. The other qubit of this second Bell-EPR pair (bottom-line) is dispatched to the destination. The sub-circuit enclosed in the large rectangle on the right does Bell-EPR measurement preparation and measurement. The behavior represented by this sub-circuit is performed by the intermediate. The intermediate dispatches the two cbits resulting from the measurement to the destination. According to the values of these cbits, the destination determines if application of Pauli gates X and Z must be done. The final result is an end-to-end Bell-EPR pair $|\Phi^+\rangle$ shared between the source and destination. The fidelity of this pair can be improved with purification. Once purified, the end-to-end Bell-EPR pair may be used to teleport a data qubit.

Several swapping operations can be used to establish entanglement between two distant terminals. It is required that dedicated memory is used to support each path. Using a routing algorithm, a path $p = v_0, v_1, \ldots, v_{s-1}, v_s$ must be chosen, where v_0 and v_s are the source and destination while s denote the length of the path, i.e., $|p|$. Entanglement is established stage by stage. For the sake of simplicity, let us assume that s is a power of two. Firstly, for $i = 0, 2, 4, \ldots, s - 2$, using vertex v_{i+1} as intermediate, entanglement swapping operation creates an entangled pair between vertices v_i and v_{i+2}. Next, for $i = 0, 4, 8, \ldots, s - 4$, using vertex v_{i+2} as intermediate, entanglement swapping creates an entangled pair between vertices v_i and v_{i+4}. Each iteration doubles the length of the segment bridged by a pair. In $\log_2 s$ iterations, an entangled pair is created between vertices v_0 and v_s.

Lemma 5. *With error probability β and fidelity $f = f(\beta)$, the end-to-end fidelity across a path $p = v_0, v_1, \ldots, v_{s-1}, v_s$ is f^s.*

---

[1]Other more advanced error models are available in the related literature, and could be considered in future work.
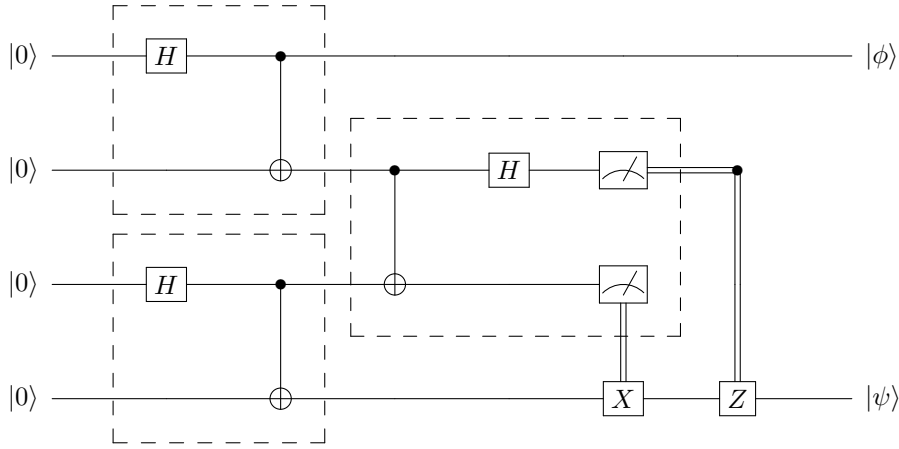
Fig. 3. Entanglement swapping.

Proof. The proof is by induction on the logarithmic (base two) length of a path.

Basis Case: ($\log_2 s$ is one). The path p consists of three vertices v_0, v_1, v_2. Using pairs between v_0, v_1 and v_1, v_2 of fidelity f, intermediate v_1 establishes two qubit pairs between v_0, v_2. They are purified into a single qubit pair of fidelity $f^2 = f^s$.

Inductive Step: ($\log_2 s$ is greater than one). Assume that for $i = \log_2 s$ fidelity is f^{2^i} is achieved for a qubit pair between vertices v_0, v_{2^i}. Let $\log_2 s$ be equal to $i + 1$. The path consists of the vertices $v_0, \ldots, v_{2^i}, \ldots, v_{2^{i+1}}$. Using pairs between v_0, v_{2^i} and $v_{2^i}, v_{2^{i+1}}$ of fidelity f^{2^i}, intermediate v_{2^i} establishes two pairs between $v_0, v_{2^{i+1}}$. They are purified into a single pair of fidelity $f^{2^i} f = f^{2i+1} = f^s$. □

Definition 6. *Let $M_P(r)$ denote the memory size in qubits of a repeater r to satisfy the demands of a complete set of paths P in the graph $G = (R, T, E)$.*

Lemma 7. *Assuming that dedicated memory is used to support each path, for any graph $G = (R, T, E)$ of repeaters and terminals and any complete set of paths P the required quantum memory size of a repeater r is equal to the sum of the lengths of the paths going through r, that is,*

$$M_P(r) = \sum_{p \in C_P(r)} |p| \text{ qubits.}$$

Proof. It is shown by induction on the logarithmic (base two) length of a path that the required number of qubits is $|p|$.

Basis Case: ($\log_2 s$ is one). A path p consists of three vertices v_0, v_1, v_2. Using two entangled qubit pairs between v_0, v_1 and two entangled qubit pairs between v_1, v_2, two entangled qubit pairs are created between v_0, v_2, purified into a single entangled qubit pair. Every vertex needs storage for two qubits.

Inductive Step: ($\log_2 s$ is greater than one). Assume that for $\log_2 s = i$, i qubit storage is needed by every node to create an entangled pair between vertices v_0, v_{2^i}. Let s be equal to $i+1$. The path consists of the vertices $v_0, \ldots, v_{2^i}, \ldots, v_{2^{i+1}}$. Using two entangled qubit pairs between v_0, v_{2^i} and two entangled qubit pairs between $v_{2^i}, v_{2^{i+1}}$, two entangled qubit pairs are created between $v_0, v_{2^{i+1}}$, purified into a single entangled

qubit pair. The first two pairs require both 2^i qubits, for a total of $2^{i+1} = s$ qubits. □

IV. GENERAL GRAPHS

Clearly, the collection of paths P selected affects the quantum memory required at repeaters. In particular, there is a tradeoff between the lengths of the paths in P (required to optimize routing between pairs of terminals) and resulting quantum memory at the repeaters. Undoubtedly, some collections of paths may be better than others thus yielding different tradeoffs. To quantify such tradeoffs, we investigate upper and lower bounds for the capacity $C_G(P)$ induced by a complete set P of paths and quantum memory required by a repeater $M_P(r)$, thus pointing to optimal path sets $P \in \mathcal{P}$.

A. Lower Bound

A simple general lower bound indicating the relation between the capacity and respective sizes of the sets of terminals and repeaters is established by the following lemma.

Lemma 8. *For any graph $G = (R, T, E)$ of repeaters and terminals ($|T| > 1$) and any complete set P of paths we have that*

$$C_G(P) \geq \left\lceil \frac{1}{|R|} \binom{|T|}{2} \right\rceil \text{ qubits.}$$

Proof. By definition, for any pair of terminals there is a path p in P connecting them, whose internal vertices are repeaters. Therefore, at least $\binom{|T|}{2}$ paths must pass through repeaters, assuming that a path between a pair of terminals t, t' is counted once. Since there are $|R|$ repeaters, by the pigeonhole principle[2], there must exist a repeater r that is traversed by at least $\frac{1}{|R|} \binom{|T|}{2}$ such paths from the set P. As a consequence, it follows that for some repeater $r \in R$, $C_P(r) \geq \left\lceil \frac{1}{|R|} \binom{|T|}{2} \right\rceil$ qubits. □

The lower bound of Lemma 8 is sufficiently strong when the number $|T|$ of terminals is large with respect to the number

---

[2] The pigeonhole principle is the following statement: If we throw I items in k bins, then there must exist a bin which has at least $\lceil I/k \rceil$ items.

$|R|$ of repeaters, otherwise it is weak. An immediate corollary concerns the number of memory qubits at the repeaters.

Corollary 9 (Minimum required quantum memory). *For any graph $G = (R, T, E)$ of repeaters and terminals and any complete set of paths P, we have that the quantum memory required by a repeater r is*

$$M_P(r) \geq \left\lceil \frac{1}{|R|} \binom{|T|}{2} \right\rceil \; qubits.$$

B. Upper Bound

In general, to examine how tight a lower bound can be, one is led to proving upper bounds. There is an upper bound obtained by merely counting all the paths passing through repeaters.

Lemma 10 (Maximum required quantum memory). *For any graph $G = (R, T, E)$ of repeaters and terminals and any complete set of paths P, we have that the quantum memory required by a repeater r satisfies*

$$M_P(r) \leq \binom{|T|}{2} \; qubits.$$

Furthermore, the total quantum memory required by all the repeaters satisfies

$$\sum_{r \in R} M_P(r) \leq \binom{|T|}{2} \cdot |R| \; qubits.$$

Proof. A complete set P comprises $\binom{|T|}{2}$ paths. In the worst case, all paths are passing through all the repeaters. $\square$

To make improvements on the maximum required quantum memory one is led to consider how known all-to-all *shortest* path algorithms for the class of graphs $G = (R, T, E)$ affect the capacity of repeaters. However, it should be noted that shortest path algorithms may not necessarily lead to repeaters of optimal capacity. If possible, one may have to go around heavily congested nodes to reduce the overall capacity, which is in our case will come at the expense of fidelity.

Subgraphs of the square grid are classes of graphs for which it is possible to explore algorithms that yield good tradeoffs. These graphs have also been studied for entanglement distribution by Perseguers [18].

V. TWO DIMENSIONAL GRID

Consider the complete $k \times k$ grid graph that has k^2 nodes. Nodes are denoted by pairs (i, j) of integers, $i, j = 1, 2, \ldots, k$. We are interested in subgraphs of the square grid consisting of the set of repeaters R and set of terminals T such as the example depicted in Fig. 4. We assume that terminals are not adjacent to each other and cannot communicate directly. Every terminal must be adjacent to at least one repeater.

A. Lower Bounds

We establish a lower bound[3] on the capacity required by a set of repeaters and terminals in a complete grid graph, i.e., all the grid edges are present. The main theorem is the following.

---

[3]We make use of the standard Big-O and Big-Ω notations for integer functions, whereby $f(x) \in O(g(x))$ (resp. $f(x) \in \Omega(g(x))$) means that for some constant $C > 0$ independent of x we have $f(x) \leq Cg(x)$ (resp. $f(x) \geq Cg(x)$, for all integers x. As usual, $\Theta(g(x)) := O(g(x)) \cap \Omega(g(x))$.
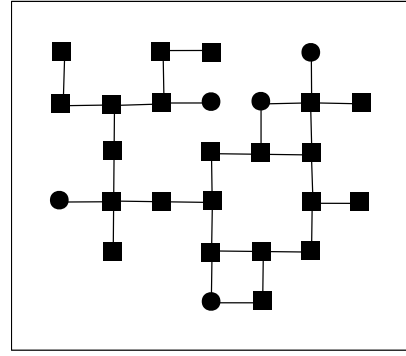

Fig. 4. A subgraph of the square grid. The squares depict repeaters (set R) and the disks terminals (set T). The set of vertices of the graph is $V = R \cup T$. The set of repeaters forms a connected subgraph. Terminals are only connected to repeaters. A terminal may be connected to more than one repeater.

Theorem 11. *For any arbitrary arrangement of repeaters and terminals in a complete $k \times k$ grid such that $|T| \in \Omega(k^{1+a})$, where $a \geq 0$ and any complete set of paths P, we have that*

$$C_G(P) \in \Omega \left(\max \left\{ k, k^{2a} \right\} \right).$$

Before proving the theorem, we state and prove two lemmas. The first lemma follows directly from Lemma 8 while in the second lemma a new argument is provided to establish a lower bound.

Lemma 12 (If $|T|$ is in $\Omega(k^{1+a})$). *For any arbitrary arrangement of repeaters and terminals in a $k \times k$ grid such that $|T| \in \Omega(k^{1+a})$ and any complete set P of paths we have that*

$$C_G(P) \in \Omega(k^{2a}) \; qubits.$$

where $a > 0$ is a constant. In particular, if $|T| \in \Omega(k^2)$ then $C_G(P) \in \Omega(k^2)$.

Proof. Applying Lemma 8, we see that that the resulting capacity of any complete set of paths must satisfy $C_G(P) \in \Omega(k^{2a})$, for any set T of terminals of size $\Theta(k^{1+a})$ and set R of repeaters. Note that a set of repeaters always has size $O(k^2)$. $\square$

Lemma 13 (If $|T|$ is in $\Omega(k)$). *For any arbitrary arrangement of repeaters and terminals in a $k \times k$ grid such that $|T| \in \Omega(k)$ and any complete set P of paths we have that*

$$C_G(P) \in \Omega(k) \; qubits.$$

Proof. Consider a set T of terminals of size $\Omega(k)$. The proof follows by considering two cases.

Case 1. If there is a vertical line, say ℓ, separating the set T into two sets T_L, T_R so that $\Omega(k)$ terminals from T are to the left of ℓ and $\Omega(k)$ terminals are to the right of ℓ then the proof is easy because the two sets must give rise to $\Omega(k^2)$ pairs of paths connecting terminals from T_L to terminals from T_R. Since the vertical lines has k nodes, by the pigeon hole principle there must exist a repeater on the line which will be traversed by $\Omega(k)$ paths. Therefore $C_G(P) \geq \Omega(k)$.

Case 2. For any vertical line ℓ separating the set T into two sets T_L, T_R (Left and Right of ℓ, respectively) not both can be of size $\Omega(k)$. Now consider the vertical line ℓ moving from left to right in the $k \times k$ grid one column at a time. At one extreme at the leftmost column, it will have zero terminals to
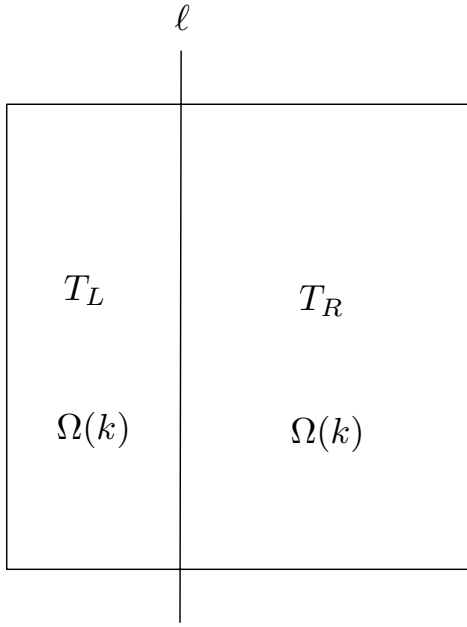
Fig. 5. In Case 1, there is a vertical line separating the set of terminal nodes into two pairwise disjoint subsets T_L, T_R each of size $\Omega(k)$.

Fig. 6. In Case 2, there are two consecutive vertical lines such that between them they separate $\Omega(k)$ terminal nodes.

its left and the remaining $\Omega(k)$ terminals to its right. Similarly, at the other extreme in the righmost column, it will have $\Omega(k)$ terminals to its left and none to its right. Furthermore, by the assumption, for any vertical column in between these two extreme positions the sizes of the sets (T_L, T_R) must be either $(\Omega(k), o(k))$ or $(o(k), \Omega(k))$, respectively. It follows there must exist a vertical line ℓ so that the sizes of (T_L, T_R) are $(\Omega(k), o(k))$, respectively, and in the next vertical line ℓ' the sizes of (T_L, T_R) are $(o(k), \Omega(k))$, respectively (see Fig. 6). Clearly, this can happen only if in the vertical column between these two lines ℓ, ℓ' there exists $\Omega(k)$ terminals.

However, if a vertical column has $\Omega(k)$ terminals there must exist a horizontal line h so that $\Omega(k)$ terminals are above h and $\Omega(k)$ are below h.

Now the rest of the proof follows from an argument similar to that of Case 1. These last two sets must give rise to $\Omega(k^2)$ pairs of paths connecting $\Omega(k)$ terminals lying above h to $\Omega(k)$ terminals lying below h, thus giving rise to $\Omega(k^2)$ paths traversing h. By the pigeonhole principle, there must a repeater which has capacity at least $\Omega(k)$. □

Proof. (Theorem 11) Depending on the size of the set of terminals T, either Lemma 21 or Lemma 13 is applicable. □

Corollary 14. *For any arbitrary arrangement of repeaters and terminals in a complete $k \times k$ grid such that $|T| \in \Omega(k^{1+a})$, where $a \geq 0$, and any complete set P of paths we have that the quantum memory required by a repeater r satisfies*

$$M(r) \in \Omega\left(\max\left\{k, k^{2a}\right\}\right) \text{ qubits.}$$

Consider a connected set of repeaters R in a $O(1) \times k$ grid. Let the associated set of terminals T be of size $\Omega(k)$.
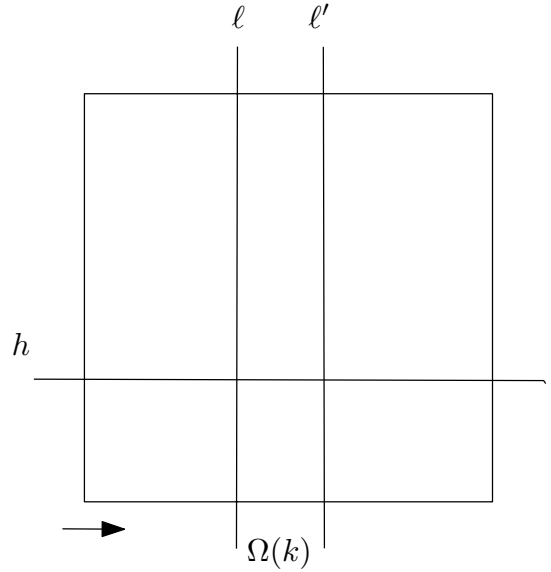
Lemma 15. *For any arbitrary arrangement of repeaters and terminals in a $O(1) \times k$ grid such that there are $|T| \in \Omega(k)$ terminals, and any complete set P of paths we have that*

$$C_G(P) \in \Omega(k^2) \text{ qubits.}$$

Proof. (Outline) Let R be the associated set of repeaters. Assume that $|T| = \Omega(k)$. Since every terminal can be adjacent to at most four repeaters, we must also have that $|R| \in \Omega(k)$. Since there is a total of $O(k)$ nodes in a $O(1) \times k$ grid, we conclude that there are $|R| \in \Theta(k)$ repeaters. Since there are $\Omega(k^2)$ paths traversing repeaters. Therefore, by the pigeon hole principle there must exist a repeater that requires capacity $\Omega(k)$. □

Corollary 16. *For any arbitrary arrangement of repeaters and terminals in a $O(1) \times k$ grid such that there are $|T| \in \Omega(k)$ terminals, and any complete set P of paths we have that the quantum memory required by a repeater r is*

$$M(r) \in \Omega(k^2) \text{ qubits.}$$

B. Upper Bounds: Three Examples

To obtain tighter bounds on the capacity of the repeaters, we employ the idea of congestion avoidance. It means to avoid shortest paths and re-route instead around highly congested nodes possibly at the expense of the fidelity of the resulting system of paths. One may say that this amounts to peeling the grid graph in layers and selecting paths along these layers so as to distribute evenly the overall load on the repeaters along the selected layers.

An elementary shortest path algorithm on a $k \times k$ grid gives an upper bound of $O(|T|^2)$. It turns out that the upper bound we can obtain depends on the number of repeaters available. We illustrate this with three examples.

Example 17. *Let us consider a grid where $|R| = |T| = k$ and $C_G(P)$ is in $\Theta(k^2)$, for any complete set of paths P.*

Consider a $2 \times k$ grid such that k terminals are in positions $(1,i), i = 1, 2, \ldots, k$, in the first row, and k repeaters are in positions $(2,i), i = 1, 2, \ldots, k$, in the second row (see Fig. 7).
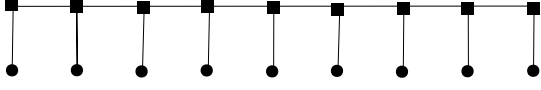

Fig. 7. A $2 \times k$ grid of k terminals (depicted as squares) and k repeaters (depicted as disks).

Without loss of generality assume that k is even ≥ 2. For each pair of terminals $(1,i)$ and $(1,j)$ such that $i < j$ consider the path

$$(1,i), (2,i), (2,i+1), \ldots, (2,j-1), (2,j), (1,j).$$

This is clearly a complete set of paths P for connecting all pairs of terminals. Furthermore, the repeater $(2, k/2)$ has capacity $\Theta(k^2)$, and therefore $C_G(P)$ is at most $O(k^2)$ qubits.

The lower bound is also of the same magnitude. Indeed, there are $\Omega(k^2)$ pairs of terminals and therefore $\Omega(k^2)$ paths are necessary to connect all such pairs of terminals. However, it is easy to see from the configuration of the $2 \times k$ grid that the repeater $(2, k/2)$ in the middle of the second row requires capacity of at least $\Omega(k^2)$ qubits.

Lemma 18. *In this example, the quantum memory required by repeater r in position $(2,i)$, $i = 1, \ldots, k/2$, is*

$$M(r) = (j-1) \cdot (k+1-j) \text{ qubits.}$$

It is therefore clear that repeaters near the middle of the $2 \times k$ grid carry the highest load as opposed to repeaters near the endpoints, which carry the lowest.

Example 19. *Let us consider a grid where $|R| = k(k-1)$, $|T| = k$ and there is a complete set of paths P such that $C_G(P)$ is in $\Theta(k)$.*

Consider a $k(k-1)$ grid consisting of $k(k-1)$ repeaters. Adjacent to the first row $\{(2,i), i = 1, 2, \ldots, k\}$ is a set of k terminal nodes $\{(1,i), i = 1, 2, \ldots, k\}$. The terminals are not connected to each other (cf. requirements in Section III, in which we defined that terminal nodes must not be adjacent to each other in the graph); further, we assume the terminal located at $(1,i)$ is connected to the repeater $(2,i)$, for $i = 1, 2, \ldots, k$.

We can construct a complete set of paths P connecting all pairs of terminals such that $C_G(P) \in O(k)$. The construction is as follows (see Fig. 8).

- *For each $i < j$, connect the terminal $(1,i)$ to the terminal $(1,j)$ using the path of repeaters on the ith column, the $k - i + 1$st row, and j-the column. This gives a total of $k - i$ paths.*

This collection of paths, say P, is clearly complete because for every pair of terminals there is a path in P connecting them. Moreover, every repeater is traversed by at most $O(k)$ of these paths. Therefore $C_G(P) \in O(k)$.

The above bound is also tight, because for any complete set of paths P it has been shown in Theorem 11 that $C_G(P)$ is in $\Omega(k)$.

Example 20. *Let us consider a grid where $|R|, |T| \in \Omega(k^2)$ and $C_G(P)$ is in $\Theta(k^2)$, for any complete set of paths P.*
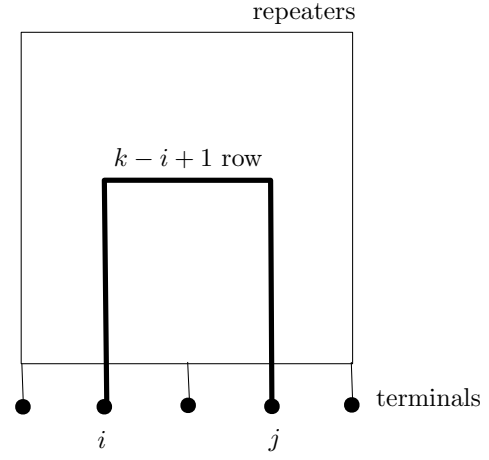

Fig. 8. A $k \times k$ grid of $(k-1)k$ terminals (not depicted) and k repeaters (depicted as disks). Depicted is the path selected between terminals $i < j$. Note that the terminals are only connected to repeaters.

We can define sets R, T each of which has size $\Theta(k^2)$. Indeed, without loss of generality assume k is even. Select the following arrangement of repeaters

$$R = \{(i,j) : i \text{ is odd and } j = 2, \ldots, k\} \cup \{(i,1) : 1 \leq i \leq k\}$$

that forms a connected subgraph. The size of R is easily seen to be $|R| = k\lceil (k+1)/2 \rceil + k/2$. Let the set of terminals be the complement of R, i.e.,

$$T = \{(i,j) : i, j = 1, 2, \ldots, k\} \setminus R.$$

The size of T is easily seen[4] to be $|T| = k^2 - k\lceil (k+1)/2 \rceil - k/2$.
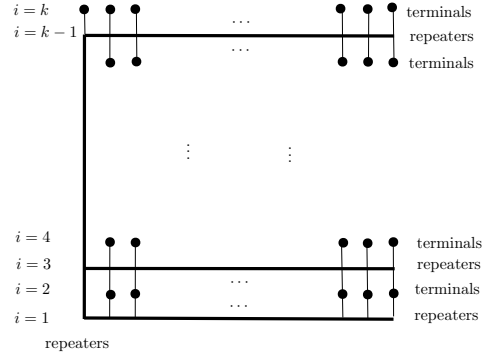
Fig. 9. A $k \times k$ grid of terminals and repeaters. Bold (normal) lines represent the respective arrays of repeaters and terminals The repeaters form a connected network while the terminals are connected only to repeaters.

C. Congestion avoidance using layer peeling

Motivated by the three main adjacency requirements defined in Section III, i.e., (1) terminal nodes must be adjacent to at least one repeater, (2) repeater nodes can communicate directly with each other if they are adjacent in the graph, and (3) terminal nodes must not be adjacent to each other in the

---

[4]For details of the construction, see Fig. 9.

graph, we present in Algorithm 1 a valid process to generate congestion avoiding paths using layer peeling. The motivation for Algorithm 1 comes from routing in planar graphs.

Algorithm 1 Path Algorithm for Planar Graphs

1: **for** each starting terminal node i **do**
2:    set $c \leftarrow i$
3:    **for** each ending terminal node j **do**
4:       *Traverse the face adjacent to i and flip faces*
5:       *at the edge where the line connecting i and j*
6:       *determine new current node c*
7:       **if** terminal node j has not been found **then**
8:          *Traverse new face*
9:       **else**
10:         *Stop*

Algorithm 2 Path Algorithm Adapted to $k \times k$ Grids

1: **for** each starting terminal node i **do**
2:    **for** each ending terminal node j **do**
3:       *Construct globally congestion avoiding paths,*
4:       *connecting i to j*

Algorithm 3 Random Arrangement of Repeaters

1: Independently of other nodes, a node of the grid is made a repeater with probability p (this forms the set R of repeaters)
2: Among the remaining nodes (which have not already become repeaters) and are adjacent to repeaters, a node independently of other nodes, is made a terminal with probability q (this forms the set T of terminals).

We can adapt the rationale of Algorithm 1 by assuming $k \times k$ grids. For instance, inspired from Example 19, we can assume a simple structure in which terminal nodes located at positions $(1, i)$ get connected to repeaters in positions $(2, k)$, for $i = 1, 2, \ldots, k$. This process represents one of the simple congestion avoidance constructions referred to in lines 3 and 4 of Algorithm 2. This new structure is especially useful when the set of repeaters is dense and the set of terminals are nicely arranged. Finally, we complement Algorithm 2 with a random arrangement of repeaters. Let $0 < p, q < 1$ be real numbers. Let terminals and repeaters be placed on a $k \times k$ grid, as defined in Algorithm 2. The process in Algorithm 3 summarizes the idea and setting. The parameters p and q in Algorithm 3 can be set in such a way that they define the density of repeaters and terminals, respectively. The parameter p can also be set in a way that ensures that the set of repeaters is connected with high probability.

In the sequel, we evaluate the approaches described in Algorithms 1, 2, and 3 using a software simulation.

VI. Simulation Results

We present simulation results that compare congestion and entanglement rates obtained with the path traversing strategies presented in Section V. We use the NetworkX python library to conduct Monte Carlo simulations. The simulation code is available online. The simulation assumes path establishment for all the terminals, i.e., end-to-end paths from every terminal to any other terminal. Two path establishment algorithms are available: shortest-path establishment and layer peeling establishment (cf. Section V-B, Algorithms 1 and 2). The random arrangement of repeaters follows the strategy presented in Algorithm 3, using Bernoulli bond percolation [23], with a probability p greater than 0.5, to ensure repeater connectivity [18].

The random arrangement of terminals depends on a probability q, which determines the selection of the remaining nodes in the grid (i.e., those nodes in the grid which are not repeaters) and satisfying the adjacency constraints defined in Section III (i.e., terminal nodes are not adjacent to each other in the grid and every terminal node is adjacent to at least one repeater). Fig. 10 pictures a sample simulation execution. It shows a representative arrangement of terminals and repeaters over a k quadratic grid graph, with values $k = 10$, $p = 0.55$ and $q = 1$. The graph contains 37 terminals, including the 32 outer ring nodes (i.e., row of nodes 1 to 8, row of nodes 91 to 98, column of nodes 10 to 80 and column of nodes 19 to 89) and five additional nodes in the inner rings (nodes 22, 35, 44, 64, 76). In our simulations, congestion and entanglement rate are computed as follows:

- **Congestion.** We compute path congestion as the number of paths passing through the most visited repeater. For instance, in Fig. 10 we can see that the most visited repeater is node 31, which appears in exactly 288 paths (out of 666 paths).

- **Entanglement Rate.** In addition to congestion, our simulations compare the entanglement rate obtained with the two path establishment algorithms (i.e., shortest-path establishment vs. layer peeling establishment). Our entanglement rate implementation follows the work of Caleffi, Uphoff and Wang [24], [25], [26], summarized next.

A. Link Entanglement Rate Calculation

In this section, we formally define the concepts of link and route entanglement rates. The assumptions regarding specific values are taken from [24], [25], [26].
Let d and $\mathcal{X}$ denote the length (m) and classical communication time (s) of an optical link. For a grid topology, they are the same across all links.

The symbol v denotes the efficiency of Bell-State Measurement (BSM), assumed to be 39%. L is the attenuation length of the optical fiber, assumed to be 22 km. The atom-photon entanglement generation probability, assumed to be 53% across all nodes, is denoted by p. Over a single link, the entanglement generation probability is defined as [25]:

$$q = \frac{vp^2}{2} e^{-d/L}$$

The constants τ_a, τ_d, τ_h, τ_o, τ_p and τ_t respectively define the atomic BSM duration, duty cycle duration for atom cooling, herald detector duration, optical BSM duration, atom pulse duration and telecom detector duration, assumed to be 10, 100, 20, 10, 5.9 and 10 μs. The time needed for an atom-photon entanglement operation is defined as

$$S = \tau_p + \max(\tau_h, \tau_t) \ \mu s.$$

```
## Initial Parameters
k = 10 #k quadratic (2D) lattice
p = 0.55 #bernoulli probability for bond percolation
q = 1 #bernoulli probability for terminal arrival

DrawGrid=True
ShowLabels=True
AdditionalRing=True
BondPercolation=True
ComputePaths=True
PathSearchAlgorithm=1 #1=shortestPaths 2=peelingPaths
CSVFormat=False
```

```
Output:
The graph contains 56 repeaters [ [11, 12, 13, 14, 15, 16, 17,
18, 21, 23, 24, 25, 26, 27, 28, 31, 32, 33, 34, 36, 37, 38, 41,
42, 43, 45, 46, 47, 48, 51, 52, 53, 54, 55, 57, 58, 61, 62, 63,
67, 68, 71, 72, 73, 74, 75, 77, 78, 81, 82, 83, 84, 85, 86, 87,
88] ] and 37 terminals [ [1, 2, 3, 4, 5, 6, 7, 8, 10, 19, 20,
29, 30, 39, 40, 49, 50, 59, 60, 69, 70, 79, 80, 89, 91, 92, 93,
94, 95, 96, 97, 98, 22, 35, 44, 64, 76] ]

Paths:
1 -> 2 : [1, 11, 12, 2]
1 -> 3 : [1, 11, 21, 31, 32, 33, 34, 24, 14, 13, 3]
...
```

```
...
22 -> 35 : [22, 21, 31, 41, 42, 43, 53, 54, 55, 45, 35]
22 -> 44 : [22, 21, 31, 41, 42, 43, 44]
22 -> 64 : [22, 21, 31, 41, 51, 61, 62, 63, 64]
22 -> 76 : [22, 21, 31, 41, 51, 61, 62, 63, 73, 74, 75, 85, 86, 76]
35 -> 44 : [35, 45, 55, 54, 53, 43, 44]
35 -> 64 : [35, 45, 55, 54, 53, 52, 51, 61, 62, 63, 64]
35 -> 76 : [35, 45, 55, 54, 53, 52, 51, 61, 62, 63, 73, 74, 75, 85, 86, 76]
44 -> 64 : [44, 43, 42, 41, 51, 61, 62, 63, 64]
44 -> 76 : [44, 43, 42, 41, 51, 61, 71, 72, 73, 74, 75, 85, 86, 76]
64 -> 76 : [64, 63, 73, 74, 75, 85, 86, 76]

Congestion = 288 (Repeater 31 appears in 288 paths, repeater 41 appears in 245 paths, repeater 51 appears in 223 paths, etc.)
Average path length is 10
```
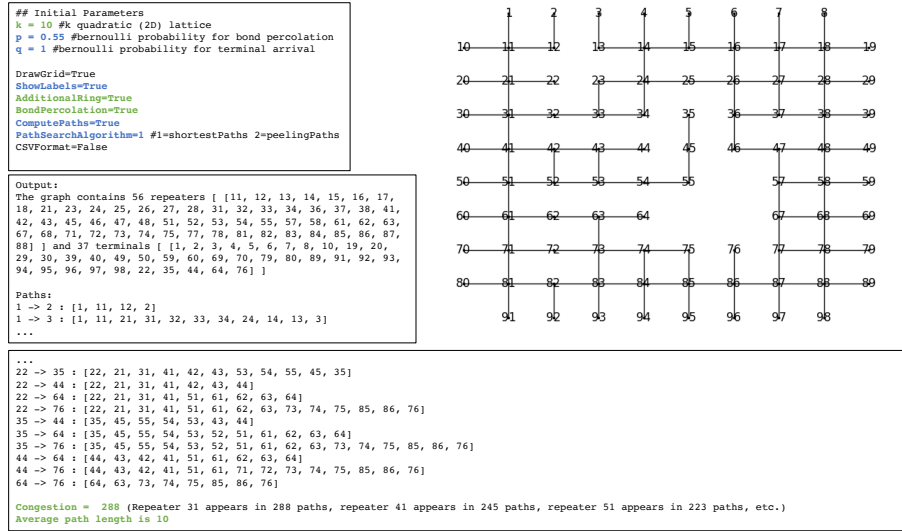
Fig. 10. Interface of our simulations, showing a sample execution run with a $k \times k$ grid of terminals and repeaters. Value of k is 10. Probabilities are set to $p = 0.55$ and $q = 1$. The simulation computes a grid graph containing 56 repeaters and 37 terminals.

Let c denote the light propagation speed, assumed to be $2 \cdot 10^5$ km/s. The time needed for an atom-photon entanglement generation and reception of an acknowledgement is

$$\tau = \tau_t + \frac{d}{2c} + \tau_o + \mathcal{X} \ \mu s.$$

The time required to perform a successful entanglement on a link is defined as:

$$\mathcal{X}_s = \tau_p + \max(\tau_h, \tau) \ \mu s.$$

The time required to perform an unsuccessful entanglement on a link is defined as:

$$\mathcal{X}_u = \tau_p + \max(\tau_h, \tau, \tau_d) \ \mu s.$$

The time needed generate entanglement between two nodes directly connected by a link is

$$S = \frac{(1-q)\mathcal{X}_u + q\mathcal{X}_s}{q} \ \mu s.$$

Let $\mathcal{X}_{ch}$ represent the quantum memory coherence time, assumed to be 10 ms. If $\mathcal{X}_{ch} \geq \tau$, then the **link entanglement rate** is
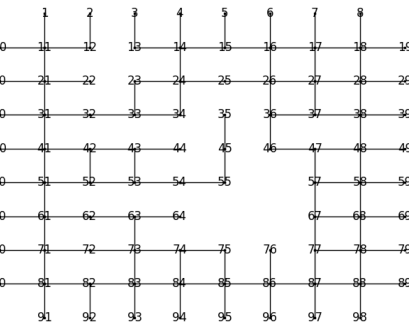
$$1/S \text{ pairs per } \mu s.$$

Otherwise, it is null.

B. Route Entanglement Rate Calculation

End-to-end entanglement builds upon entanglement swapping. We review a performance model for end-to-end entanglement on a route. For a route of length n (links), the classical communication time between the two endpoints of the route is equivalent to

$$C(n) = n \cdot \mathcal{X} \ \mu s.$$

Let v_a denote the atomic BSM efficiency, assumed to be 10 μs and 39%. On a route of length n, entanglement time is recursively defined as:

$$R(n) = \begin{cases} 0, \text{ if } n = 0 \\ S\mu s, \text{ if } n = 1 \\ \frac{R(k) + \tau_a + C(k)}{v_a}\mu s, \text{ if } n > 1 \text{ with } k = \lceil \frac{n}{2} \rceil \end{cases}$$

Lemma 21. *The time complexity of route entanglement is $n \log(n)$.*

Entanglement is attempted in rounds until it succeeds. On a route of length n, the duration of the last round, i.e., the successful one, is defined as follows:

$$\tau(n) = \begin{cases} 0, \text{ if } n = 0 \\ \mathcal{X}_s \mu s, \text{ if } n = 1 \\ \tau(k) + \tau_a + C(k)\mu s, \text{ if } n > 1 \text{ with } k = \lceil \frac{n}{2} \rceil \end{cases}$$

The **route entanglement rate** (qubit pairs per μs) is:

$$\mathcal{T}(n) = \begin{cases} 1/R(n), \text{ if } \mathcal{X}_{ch} \geq \tau(n) - (\mathcal{X}_s - \tau(1)) \\ 0, \text{ else} \end{cases}$$

C. Monte Carlo Simulation Results

Fig. 11 provides the results with regard to congestion. Boxplots in Fig. 11(a,c) provide, respectively, the results when we apply the shortest-path algorithm. Boxplots in Fig. 11(b,d) provide the results when we apply the layer-peeling path algorithm. Every Boxplot corresponds to fifty independent run executions per algorithm. Values of p and q are 0.95 in Fig. 11(a,b); and 0.65 in Fig. 11(c,d). Fig.12 provide the entanglement rate results using the same rationale. We can observe that the layer-peeling algorithm improves (i.e., reduces) the network congestion w.r.t. the use of a shortest-path algorithm. Nevertheless, the entanglement rate remains similar for both cases.
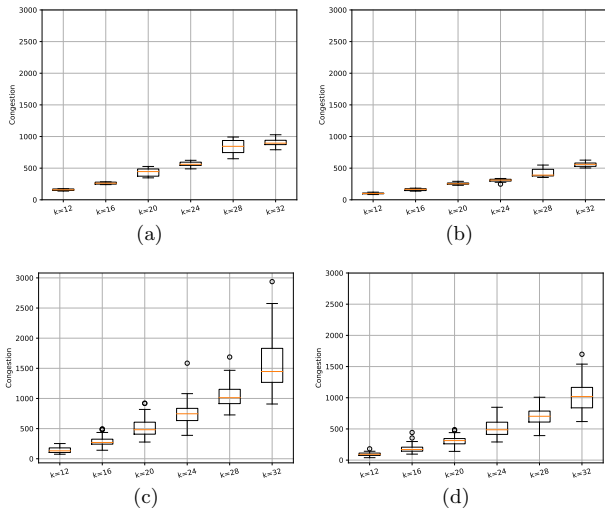
Fig. 11. Congestion results using (a,c) shortest path and (b,d) peeling path strategies. Values of p and q are 0.95 in (a,b) and 0.65 in (c,d).
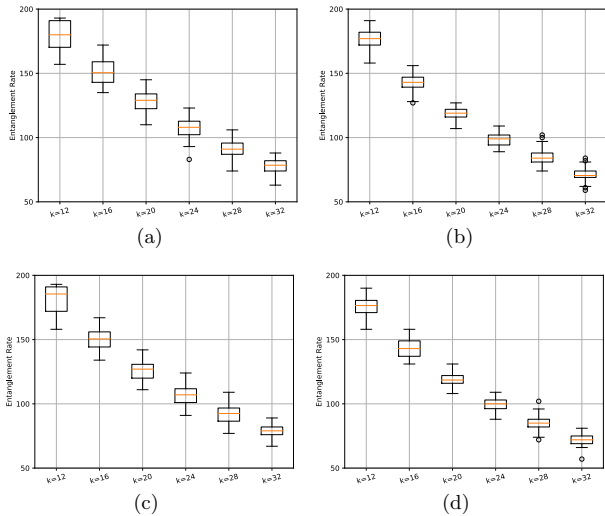

Fig. 12. Entanglement rate results using (a,c) shortest path and (b,d) peeling path strategies. Values of p and q are 0.95 in (a,b) and 0.65 in (c,d).

VII. CONCLUSION

We have explored path congestion avoidance in quantum communication networks. We have assumed networks of repeaters and terminals in which the sets of complete paths between terminals may affect the capacity of repeaters in the network. We have compared the reduction of avoidance of two representative path establishment algorithms: shortest-path establishment vs. layer-peeling path establishment. We have observed that both strategies provide an equivalent entanglement rate, while the layer-peeling establishment algorithm considerably reduces the congestion in the network of repeaters. Repeaters in the inner layers get less congested and would require a lower number of qubits, while providing a similar entanglement rate.

REFERENCES

[1] W. J. Munro, K. A. Harrison, A. M. Stephens, S. J. Devitt, and K. Nemoto, "From quantum multiplexing to high-performance quantum networking," *Nature Photonics*, vol. 4, no. 11, pp. 792–796, 2010. [Online]. Available: https://doi.org/10.1038/nphoton.2010.213

[2] L. Jiang, J. M. Taylor, K. Nemoto, W. J. Munro, R. Van Meter, and M. D. Lukin, "Quantum repeater with encoding," *Phys. Rev. A*, vol. 79, p. 032325, Mar 2009.

[3] P. Mazurek, A. Grudka, M. Horodecki, P. Horodecki, J. Łodyga, Ł. Pankowski, and A. Przysieżna, "Long-distance quantum communication over noisy networks without long-time quantum memory," *Phys. Rev. A*, vol. 90, p. 062311, Dec 2014. [Online]. Available: https://link.aps.org/doi/10.1103/PhysRevA.90.062311

[4] C. Simon, "Towards a global quantum network," *Nature Photon*, vol. 11, pp. 678––680, 2017.

[5] R. Van Meter, *Quantum Networking*, ser. ISTE. Wiley, 2014. [Online]. Available: https://books.google.ca/books?id=khmNAwAAQBAJ

[6] S. Wehner, D. Elkouss, and R. Hanson, "Quantum internet: A vision for the road ahead," *Science*, vol. 362, no. 6412, 2018. [Online]. Available: https://science.sciencemag.org/content/362/6412/eaam9288

[7] C. H. Bennett, G. Brassard, C. Crépeau, R. Jozsa, A. Peres, and W. Wootters, "Teleporting an unknown quantum state via dual classical and einstein-podolsky-rosen channels," *Phys. Rev. Lett.*, vol. 70, pp. 1895–1899, Mar 1993. [Online]. Available: http://link.aps.org/doi/10.1103/PhysRevLett.70.1895

[8] M. Żukowski, A. Zeilinger, M. A. Horne, and A. K. Ekert, ""event-ready-detectors" bell experiment via entanglement swapping," *Phys. Rev. Lett.*, vol. 71, pp. 4287–4290, Dec 1993. [Online]. Available: http://link.aps.org/doi/10.1103/PhysRevLett.71.4287

[9] R. Van Meter, T. Satoh, T. D. Ladd, W. J. Munro, and K. Nemoto, "Path selection for quantum repeater networks," *Networking Science*, vol. 3, no. 1, pp. 82–95, 2013. [Online]. Available: http://dx.doi.org/10.1007/s13119-013-0026-2

[10] H.-J. Briegel, W. Dür, J. I. Cirac, and P. Zoller, "Quantum repeaters: The role of imperfect local operations in quantum communication," *Phys. Rev. Lett.*, vol. 81, pp. 5932–5935, Dec 1998. [Online]. Available: https://link.aps.org/doi/10.1103/PhysRevLett.81.5932

[11] K. Azuma, K. Tamaki, and H. Lo, "All-photonic quantum repeaters," *Nature Communications*, vol. 6, no. 6787, pp. 1–7, 2015.

[12] W. J. Munro, K. Azuma, K. Tamaki, and K. Nemoto, "Inside quantum repeaters," *IEEE Journal of Selected Topics in Quantum Electronics*, vol. 21, no. 3, pp. 78–90, May 2015.

[13] S. Bäuml, K. Azuma, G. Kato, and D. Elkouss, "Linear programs for entanglement and key distribution in the quantum internet," 2018.

[14] L. Gyongyosi and S. Imre, "Decentralized base-graph routing for the quantum internet," *Phys. Rev. A*, vol. 98, p. 022310, Aug 2018. [Online]. Available: https://link.aps.org/doi/10.1103/PhysRevA.98.022310

[15] M. Pant, H. Krovi, D. Towsley, L. Tassiulas, L. Jiang, P. Basu, D. Englund, and S. Guha, "Routing entanglement in the quantum internet," *npj Quantum Information*, vol. 5, no. 1, p. 25, 2019. [Online]. Available: https://doi.org/10.1038/s41534-019-0139-x

[16] S. Pirandola, "End-to-end capacities of a quantum communication network," *Communications Physics*, vol. 2, no. 1, p. 51, 2019. [Online]. Available: https://doi.org/10.1038/s42005-019-0147-3

[17] M. Caleffi, "Optimal routing for quantum networks," *IEEE Access*, vol. 5, pp. 22 299–22 312, 2017.

[18] S. Perseguers, "Entanglement distribution in quantum networks," Ph.D. dissertation, Technische Universität München, 2010.

[19] E. Schoute, L. Mancinska, T. Islam, I. Kerenidis, and S. Wehner, "Shortcuts to quantum network routing," 2016.

[20] L. Jiang, J. M. Taylor, N. Khaneja, and M. D. Lukin, "Optimal approach to quantum communication using dynamic programming," *Proceedings of the National Academy of Sciences*, vol. 104, no. 44, pp. 17 291–17 296, 2007. [Online]. Available: https://www.pnas.org/content/104/44/17291

[21] E. Shchukin, F. Schmidt, and P. van Loock, "Waiting time in quantum repeaters with probabilistic entanglement swapping," *Phys. Rev. A*, vol. 100, p. 032322, Sep 2019.

[22] M. Shirichian and S. Tofighi, "Protocol for routing entanglement in the quantum ring network," in *2018 9th International Symposium on Telecommunications (IST)*, Dec 2018, pp. 658–663.

[23] H. Duminil-Copin, "Introduction to bernoulli percolation," 2018.

[24] M. Caleffi, "Optimal routing for quantum networks," *IEEE Access*, vol. 5, pp. 22 299–22 312, 2017.

[25] M. Uphoff, M. Brekenfeld, G. Rempe, and S. Ritter, "An integrated quantum repeater at telecom wavelength with single atoms in optical fiber cavities," *Applied Physics B*, vol. 122, no. 3, p. 46, 2016.

[26] Y. Wang, M. Um, J. Zhang, S. An, M. Lyu, J.-N. Zhang, L.-M. Duan, D. Yum, and K. Kim, "Single-qubit quantum memory exceeding ten-minute coherence time," *Nature Photonics*, vol. 11, no. 10, pp. 646–650, 2017.